Phospholipid-Dependent Regulation of Cytochrome c_3-Mediated Electron Transport across Membranes

Suhk-mann Kim,* Toshinori Yamamoto,* Yasuto Todokoro,† Yuki Takayama,† Toshimichi Fujiwara,† Jang-Su Park,† and Hideo Akutsu†

*Faculty of Engineering, Yokohama National University, Yokohama 240-8501, Japan; and †Institute for Protein Research, Osaka University, Suita 565-0871, Japan

ABSTRACT Cytochrome c_3 (cyt c_3) can mediate electron transport across phosphatidylcholine (PC)/cardiolipin (CL) and PC/phosphatidylglycerol (PG) membranes. A two-molecule process is involved in the electron transport across PC/CL membranes in the liquid-crystalline state. In contrast, a single-molecule process dominates the electron transport across PC/CL membranes in the gel state and PC/PG membranes in the liquid-crystalline and gel states. Namely, the electron transport mechanism differs with the phospholipid composition and membrane fluidity. The rate-limiting step of the two-molecule process was lateral diffusion of cyt c_3 in membranes. The rate constants for the three single-molecule process cases were similar to each other. To elucidate these reaction processes, interactions between cyt c_3 and phosphate groups and between cyt c_3 and the glycerol backbones of phospholipid bilayers were investigated by means of ^{31}P and ^{2}H solid-state NMR, respectively, for CL and PC/CL membranes. The results showed that the polar headgroups of both phosphatidylcholine and CL are involved in the binding of cyt c_3. Also, cyt c_3 penetrates into membranes, which would induce distortion of the lipid bilayer. The molecular mechanisms underlying the single- and two-molecule processes are discussed in terms of membrane structure.

INTRODUCTION

Cytochrome c_3 (cyt c_3) from *Desulfovibrio vulgaris* Miyazaki F (*Dv*MF) consists of four hemes and a single polypeptide chain. It is involved in the electron-transport system for sulfate respiration and is located in the periplasm of sulfate-reducing bacteria (1). Extensive work has been carried out on this protein because of its unique properties (1–3). The crystal structure of *Dv*MF cyt c_3 at 0.11 nm resolution is now available (4). Its redox behavior has been extensively investigated through NMR and electrochemical studies (3,5,6), and thereby the microscopic redox potentials of cyt c_3 were determined.

Cyt c_3 was reported to bind to lipid membranes, including cardiolipin (CL), and to be involved in electron transport across membranes (7–9). In contrast, cytochrome *c* (cyt *c*) could not mediate electron transport across the membranes (7). However, the mechanism underlying the electron transport across these membranes has not been clarified. To elucidate the mechanism, electron transport kinetics were extensively investigated in terms of membrane fluidity and phospholipid composition in this work. Furthermore, interactions between cyt c_3 and phospholipid membranes were analyzed by solid-state NMR. Although there have been a number of studies on cyt *c*-membrane interactions ((10–12) and references therein), there have only been a few for cyt c_3 (13). We previously reported a ^{2}H and ^{31}P solid-state NMR study on the interactions of ferro- and ferri-cytochrome c with phospholipid membranes including CL (14). Similar techniques were employed in this work. The investigation has revealed that the mode of electron transport mediated by cyt c_3 differs with the phospholipid composition and membrane fluidity. The molecular mechanism of electron transport across membranes was discussed on the basis of cyt c_3-membrane interactions.

MATERIALS AND METHODS

Preparation of cyt c_3

*Dv*MF cells were cultured at 37°C in Postgate C medium (2). Cyt c_3 was purified from *Dv*MF cells according to the reported method (15,16). Its purity was confirmed by sodium dodecyl sulfate-polyacrylamide gel electrophoresis. The purity index (A_{552}(red)/A_{280}(ox)) of the purified sample was >3.0. Absorption spectra were obtained with a Shimadzu UV-2000 spectrophotometer (Kyoto, Japan).

Phospholipids and specific deuteration of the glycerol moiety of cardiolipin

Cardiolipin from beef heart (beefCL), 1,2-dimyristoyl-*sn*-glycero-3-phosphocholine (dmPC), egg phosphatidylcholine (eggPC), 1,2-dimyristoyl-*sn*-glycero-3-phosphoglycerol (dmPG), and 1,2-dioleoyl-*sn*-glycero-3-phosphocholine (doPC) were purchased from Sigma (St. Louis, MO). Their purity was checked by thin layer chromatography. Phosphatidylcholine (coliPC) was synthesized by methylation of PE purified from *Escherichia coli* cells (17). Phosphatidylglycerol (eggPG) was synthesized from eggPC by one-step transphosphatidylation catalyzed by phospholipase D in the presence of glycerol (18). The synthesis of perdeuterated glycerol ([$^{2}H_5$]-glycerol) was performed as described elsewhere (19). The deuterated

Submitted April 26, 2005, and accepted for publication October 11, 2005.

Address reprint requests to Hideo Akutsu, Institute for Protein Research, Osaka University 3-2 Yamadaoka, Suita 565-0871, Japan. Tel.: 06-6879-8597; Fax: 06-6879-8599; E-mail: akutsu@protein.Osaka-u.ac.jp.

Suhk-mann Kim's present address is Dept. of Physics, Pusan National University, Busan 609-735, Korea.

Jang-Su Park's present address is Dept. of Chemistry, Pusan National University, Busan 609-735, Korea.

0006-3495/06/01/506/08 $2.00

doi: 10.1529/biophysj.105.065359

glycerol was incorporated into the cells of an *E. coli* mutant requiring glycerol (*E. coli* K-12 GRA) at 37°C. Phosphatidylethanolamine (coliPE) and cardiolipin (coliCL) were extracted from the mutant cells according to the reported method (19).

Preparation of cyt c_3-bound single-bilayer liposomes

Single-bilayer liposomes (referred to as vesicles hereafter) were prepared according to the reported method (9). Eighty milligrams of PC and 20 mg of CL or PG were dissolved in 10 mL of chloroform, and then the solution was dried to a film. It was further dried under high vacuum to remove all traces of organic solvent. The dried lipid film was suspended in 5 mL of a 0.5 M $K_3Fe(CN)_6$, 5 mM Tris-HCl (pH 7.4) solution, and then the suspension was sonicated (5 min × 6; Branson Sonifier 250, Danbury, CT) under a nitrogen gas flow with external ice cooling. The suspension was centrifuged at 20,000 rpm (Hitachi CP-70 Ultracentrifuge, rotor RP-30, Hitachi, Japan) for 30 min at 4°C. To separate vesicles from free $K_3Fe(CN)_6$ and multilamellar liposomes, the supernatant was loaded on a Sepharose 4B column (30 mm × 350 mm) at 4°C and then eluted with a 5 mM Tris-HCl (pH 7.4) solution. The vesicles gave an absorption band at 419 nm, which is characteristic of $K_3Fe(CN)_6$. This was used to determine the concentration of the vesicles. The phospholipid concentration was determined for vesicles without $K_3Fe(CN)_6$ by the method of Gerlach and Deuticke (20).

A desired amount (0.05–0.33 mL) of a 120 μM cyt c_3 solution was added drop-wise to a freshly prepared vesicle solution with gentle stirring at room temperature. Then, free cyt c_3 was removed from the cyt c_3-bound vesicles by washing on a filter, YM-100 (Amicon, Beverly, MA), with a degassed 5 mM Tris-HCl buffer (pH 7.4) solution at 4°C. The concentration of cyt c_3 was determined using the absorption at 552 nm ($\varepsilon = 119\ mM^{-1}cm^{-1}$ (21)) after complete reduction.

Measurement of redox kinetics

A total of 0.95 mL of the cyt c_3-bound vesicle solution was put in a cell sealed with a rubber septum. The gas phase was replaced by Ar gas. The solution was mixed with 50 μL of a freshly prepared 17.2 mM $Na_2S_2O_4$ solution in a degassed 5 mM Tris-HCl buffer (pH 7.4) solution. The final $Na_2S_2O_4$ concentration was 0.86 mM. The reduction of internal $K_3Fe(CN)_6$ was monitored using the absorbance at 432 nm as a function of time. The wavelength 432 nm is the isosbestic point for the spectra of oxidized and reduced cyt c_3. The solution temperature was controlled with a thermostatic cell holder (TCC-240A, Shimadzu, Kyoto, Japan).

Preparation of NMR samples

Phospholipids were dissolved in chloroform/methanol (1:1, v/v) and then washed with 0.5 volumes of a 0.5 M Na_2SO_4, 2.0 mM EDTA (pH 7.2) solution to remove polyvalent metal ions. The chloroform fraction was dried to a film under a nitrogen gas flow. It was further dried under high vacuum overnight to remove all traces of organic solvent. Multilamellar liposomes were prepared by rigorously dispersing the dry lipid film in 5–10-fold of a 5 mM Tris-HCl (pH 7.4) solution with and without cyt c_3 (~4 mM) in deuterium-depleted water (<0.2 ppm; CEA, Paris, France) at 50°C. The dispersion was centrifuged at 3,000 rpm (Tomy TS-7 rotor, Tokyo, Japan) at 4°C, and the supernatant was removed. The precipitate was used for NMR measurements. Typically, ~40 mg of deuterated lipid was used for a ^2H NMR measurement. Sample preparation was carried out under a nitrogen atmosphere to prevent the oxidation of lipids.

NMR measurements

Solid-state ^{31}P NMR spectra were recorded with a Chemagnetics (Fort Collins, CO) CMX-400 NMR spectrometer operating at 161.15 MHz with proton decoupling. Magic-angle sample spinning (MAS) ^{31}P NMR spectra were obtained with a Varian Infinity plus CMX-500 NMR spectrometer operating at 202.28 MHz, using a MAS probe head for a 4 mm ϕ sample rotor (Walnut Creek, CA). The ^1H decoupling power was 50 kHz, and the 90° pulse width was 5 μs for ^{31}P. The recycle time was 3 s. The phosphorus chemical shifts are expressed relative to 85% phosphoric acid. Solid-state ^2H NMR spectra were obtained with the Chemagnetics CMX-400 NMR spectrometer operating at 61.1 MHz, using a MAS probe head for a 5 mmϕ sample rotor. The measurements were performed without sample rotation. The 90° pulse width was 5 μs. A quadrupole echo pulse sequence (90_x-τ_1-90_y-τ_2) was employed with $\tau_1 = 30\ \mu s$, $\tau_2 = 20\ \mu s$, and a recycle time of 0.5 s. The line broadening factor used was 100 Hz.

RESULTS

Electron transport across cyt c_3-bound membranes in single-bilayer liposome (vesicle) systems

The electron transport kinetics across cyt c_3-bound membranes in eggPC/beefCL vesicles were reported by Tabushi et al. (7–9). They characterized the system in detail. The kinetics of $Fe(CN)_6^{3-}$ reduction by $S_2O_4^{2-}$ were described as follows (9):

$$-d[Fe(CN)_6^{3-}]/dt = k[Fe(CN)_6^{3-}][S_2O_4^{2-}]^{1/2} \quad (1)$$

Fig. 1 shows the time course of the absorbance at 432 nm of $Fe(CN)_6^{3-}$ in cyt c_3-bound eggPC/beefCL (4:1 by weight) vesicles on reduction by $Na_2S_2O_4$. In our case, the initial concentrations of $Fe(CN)_6^{3-}$ and $S_2O_4^{2-}$ were 0.26 and 0.86 mM, respectively. The vesicle concentration estimated from the phosphorus quantity (typically 0.9 mM) was 0.34 μM, assuming aggregation number 2678 (9). The electron transport was suppressed in the later stage in Fig. 1, presumably because of an electric imbalance across a membrane. Thus, only the curve at the early stage was analyzed as a pseudo first-order reaction. Since the change in $[S_2O_4^{2-}]$ is small in the range analyzed, Eq. 1 can be written as

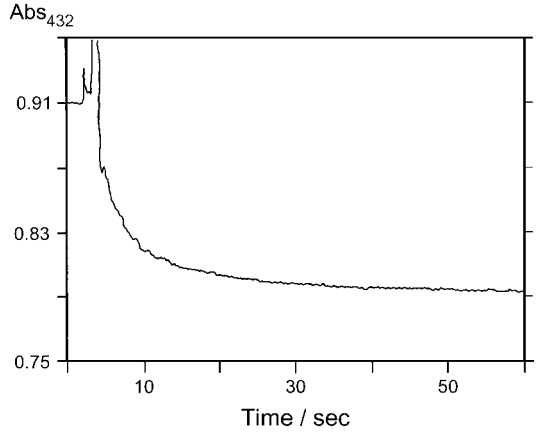

FIGURE 1 Time course of $Fe(CN)_6^{-3}$ reduction in cyt c_3-bound eggPC/beefCL vesicles with dithionite at 24°C.

$$-d[\mathrm{Fe(CN)}_6^{3-}]/\mathrm{dt} = k_1[\mathrm{Fe(CN)}_6^{3-}] \quad (2)$$

To obtain real k_1, the rate due to leaking of $\mathrm{Fe(CN)}_6^{3-}$ and $S_2O_4^{2-}$ across the membrane (k_0) should be subtracted from the observed rate (k_{app}). Thus,

$$k_1 = k_{app} - k_0 \quad (3)$$

The reduction of $\mathrm{Fe(CN)}_6^{3-}$ in vesicles without cyt c_3 was $k_0 = 0.001\ s^{-1}$. This is in good agreement with the value obtained by Tabushi et al., which shows that the vesicles were well sealed. Every kinetic data set could be analyzed in this way. The obtained k_1 is plotted as a function of the square of the cyt c_3 concentration in Fig. 2 for 4°C, 15°C, and 24°C. Since the phase transition temperature of this membrane is lower than 0°C, the lipid bilayers took the liquid-crystalline phase at these temperatures. As can be seen in Fig. 2, the observed rate constants fall on a linear line. This is in good agreement with the results reported by Tabushi et al. (7,9), who stated

$$k_1 = k_3[\mathrm{cyt}\,c_3]^2 + k_2[\mathrm{cyt}\,c_3] \quad (4)$$

and

$$k_3 \gg k_2 \quad (5)$$

This indicates that the electron transport across PC/CL membranes in the liquid-crystalline state involves two cyt c_3 molecules. Actually, most vesicles carry more than two cyt c_3 molecules under the experimental conditions used. The temperature dependence in Fig. 2 shows that the electron transport gets faster at a higher temperature, suggesting that the rate-limiting step is the encounter between two cyt c_3 molecules governed by their lateral diffusion in membranes.

To confirm the active role of cyt c_3 in the electron transport, $K_3Fe(CN)_6$ was replaced by methylviologen. The redox potential of the latter is −446 mV (22), which is much lower than that of cyt c_3 (−260 ~ −360 mV) (6). Therefore, cyt c_3 cannot reduce methylviologen, which would suppress the electron transport across membranes. Actually, dithionite could not reduce methylviologen in this system (data not shown), confirming the essential role of cyt c_3 in mediating electron transport across membranes. Furthermore, electron transport in cyt c-bound eggPC/beefCL vesicles was also examined. Cyt c could not mediate electron transport across membranes, as reported by Tabushi et al. (7). This fact also supports the conclusion that the electron transport across the cyt c_3-bound PC/CL or PC/PG membranes is actually mediated by cyt c_3.

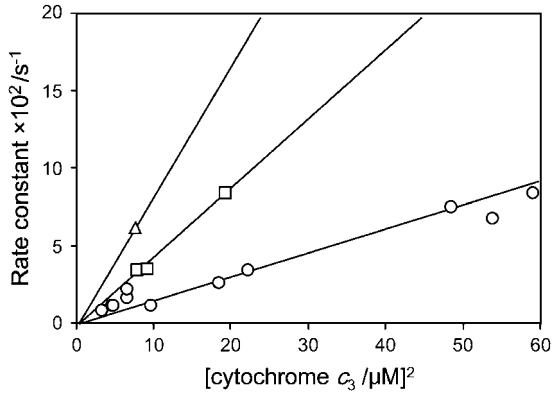

FIGURE 2 Pseudo-first-order reduction rate constants (k_1) as a function of the square of the cyt c_3 concentration in eggPC/beefCL vesicles. Lipid membranes are in the liquid crystalline state at the temperatures examined. (○), 4°C; (□), 15°C; and (△), 24°C.

Effect of membrane fluidity on the electron transport mechanism

To analyze the electron transport kinetics in the gel state, eggPC was replaced by dmPC. A thermogram of dmPC/beefCL bilayers obtained with a differential scanning calorimeter showed a broad but clear phase transition from 18°C to 23°C (data not shown). Therefore, the experiment was carried out at 4°C and 15°C, namely, in the gel state. The obtained rate constants at different cyt c_3 concentrations are summarized in Fig. 3 and Table 1. In contrast to in the liquid-crystalline state, the electron transport rate is proportional to the cyt c_3 concentration, showing that a single cyt c_3 molecule is involved in the electron transport across PC/CL membranes in the gel state, namely, $k_2 \gg k_3$ in Eq. 4. Furthermore, the second-order rate constant showed no temperature dependence (Fig. 3). Thus, it can be concluded that in cyt c_3-bound PC/CL vesicles, cyt c_3 mediates electron transport across membranes, but that the reaction process changes depending on the membrane fluidity.

Effects of acidic phospholipid species on the electron transport mechanism

The role of acidic phospholipids in the electron transport was investigated by measuring the kinetics for cyt c_3-bound

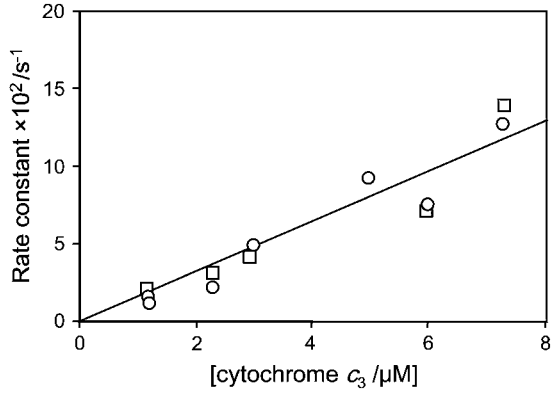

FIGURE 3 Pseudo-first-order reduction rate constants (k_1) as a function of the cyt c_3 concentration in dmPC/beefCL vesicles. Lipid membranes are in the gel state at the temperatures examined. (○), 4°C, and (□), 15°C.

TABLE 1 Electron transport rate constants across cytochrome c_3-bound membranes for the eggPC/eggPG, dmPC/dmPG, and dmPC/beefCL vesicle systems

[cyt c_3]/μM	Temp/°C	k_1/s^{-1}	(k_1/[cyt c_3])/s^{-1}M^{-1}
eggPC/eggPG	(Liquid-crystalline state)		
1.70	4	2.6×10^{-2}	1.6×10^{4}
1.88	4	3.0×10^{-2}	1.6×10^{4}
2.08	4	2.9×10^{-2}	1.4×10^{4}
2.27	4	3.4×10^{-2}	1.5×10^{4}
3.69	4	6.7×10^{-2}	1.8×10^{4}
4.38	4	8.6×10^{-2}	2.0×10^{4}
5.63	4	9.4×10^{-2}	1.7×10^{4}
6.58	4	9.4×10^{-2}	1.4×10^{4}
7.04	4	10.2×10^{-2}	1.4×10^{4}
8.32	4	10.0×10^{-2}	1.2×10^{4}
8.35	4	10.1×10^{-2}	1.2×10^{4}
9.75	4	16.6×10^{-2}	1.7×10^{4}
3.91	10	5.2×10^{-2}	1.3×10^{4}
1.47	24	2.7×10^{-2}	1.9×10^{4}
3.99	24	3.9×10^{-2}	1.0×10^{4}
4.01	24	5.4×10^{-2}	1.4×10^{4}
dmPC/dmPG	(Gel state)		
1.47	4	3.5×10^{-2}	2.4×10^{4}
3.29	4	5.9×10^{-2}	1.8×10^{4}
3.38	4	5.6×10^{-2}	1.7×10^{4}
5.98	4	12.9×10^{-2}	2.2×10^{4}
7.22	4	15.8×10^{-2}	2.2×10^{4}
1.24	15	3.0×10^{-2}	2.5×10^{4}
3.72	15	5.7×10^{-2}	1.5×10^{4}
dmPC/beefCL	(Gel state)		
1.16	4	1.6×10^{-2}	1.4×10^{4}
1.17	4	1.2×10^{-2}	1.0×10^{4}
2.28	4	2.2×10^{-2}	1.0×10^{4}
2.98	4	5.0×10^{-2}	1.7×10^{4}
4.96	4	9.2×10^{-2}	1.9×10^{4}
5.97	4	7.6×10^{-2}	1.3×10^{4}
7.26	4	12.8×10^{-2}	1.8×10^{4}
1.13	15	2.2×10^{-2}	1.9×10^{4}
2.28	15	3.2×10^{-2}	1.4×10^{4}
2.90	15	4.1×10^{-2}	1.4×10^{4}
5.94	15	7.2×10^{-2}	1.2×10^{4}
7.28	15	14.0×10^{-2}	1.9×10^{4}

eggPC/eggPG (4:1 by weight) and dmPC/dmPG (4:1) vesicles. The former and latter were used to determine the electron transport rate across PC/PG membranes in the liquid-crystalline and gel states, respectively. The obtained rate constants are summarized in Table 1 along with those for the PC/CL system in the gel state. In contrast to the case of PC/CL membranes, the rate constant was proportional to the cyt c_3 concentration in both the liquid-crystalline and gel states, namely, $k_2 \gg k_3$ in Eq. 4. No temperature dependence was observed in either state. Furthermore, the rate constants for PC/PG membranes in the gel state were similar to those in the liquid-crystalline state and also similar to those for PC/CL membranes in the gel state (Table 1). These results lead to the conclusion that the electron transport mechanism depends not only on the membrane fluidity but also on the acidic phospholipid species.

Characterization of cyt c_3-membrane interactions in multilamellar liposomes

To elucidate the different electron transport mechanisms, investigation of the interaction between cyt c_3 and phospholipid bilayers is important. This was carried out for PC/CL and CL membranes, respectively, by means of ^{31}P and ^{2}H solid-state NMR. For this purpose, we had to use multilamellar liposomes to suppress rotational motion. Although sonicated vesicles exhibit greater curvature in lipid bilayers, the essential features of the cyt c_3-membrane interaction should be common to cyt c_3-bound vesicles and multilamellar liposomes.

For characterization of NMR samples, the amount of protein bound to multilamellar liposomes was determined from the amount of protein remaining in the supernatant. The binding was strong and stable, as was seen for the preparation of cyt c_3-bound vesicles. Therefore, the binding should be almost saturated. The amounts of cyt c_3 bound to multilamellar liposomes including CL from *E. coli* cells (coliCL) are summarized in Table 2 as the molar ratio of protein/CL. The amounts of cyt c_3 bound to coliPC/coliCL and coliPE/coliCL liposomes were more or less similar to each other. They were also similar to the amounts of cyt c bound to coliPC/coliCL and coliPE/coliCL liposomes, respectively (14). Therefore, the amount of membrane-bound cyt c_3 does not depend on the species of dipolar phospholipids. However, the amount of cyt c_3 bound to the CL membranes was much less than that mentioned above. This suggests that binary phospholipid membranes are more efficient than simple CL membranes for the binding of cyt c_3. As can be seen in Table 2, the lipid/protein molecular ratios in the NMR samples were 29 and 90 for coliCL and coliPC/coliCL liposomes, respectively.

Characterization of cyt c_3-membrane interactions by solid-state ^{31}P NMR

To monitor polymorphic structures and the effect of cyt c_3 binding on polar headgroups, solid-state ^{31}P NMR spectra were obtained for coliCL and coliPC/coliCL liposomes in the absence and presence of bound cyt c_3. The spectra measured at 30°C are presented in Fig. 4. The powder pattern indicates that most phospholipids took on the liquid-crystalline lamellar phase for all samples. However, an isotropic

TABLE 2 Amounts of cytochrome c_3 bound to phospholipid membranes

Complex	molar ratio of bound cyt c_3/cardiolipin
CL-Cyt c_3	0.034
(PE/CL)-Cyt c_3	0.085
(PC/CL)-Cyt c_3	0.103

CL, cardiolipin from *E. coli*; PE, phosphatidylethanolamine from *E. coli*; PC, phosphatidylcholine synthesized from *E. coli* PE; cyt c_3, cytochrome c_3. PC/CL, for example, stands for the liposomes formed with a binary mixture of PC and CL (4:1 w/w).

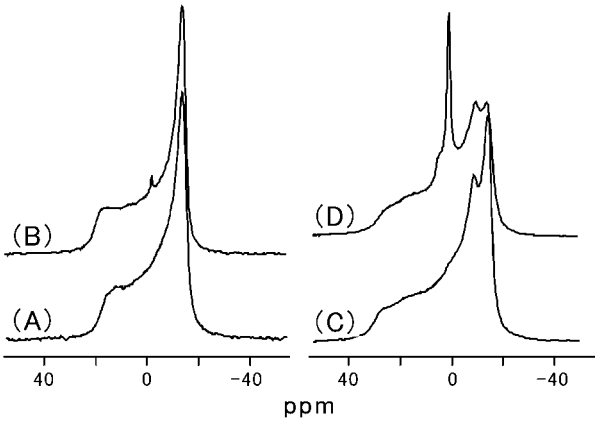

FIGURE 4 Proton decoupled ^{31}P NMR spectra of coliCL and coliPC/coliCL membranes at 161.15 MHz and 30°C. (*A*) coliCL membranes, (*B*) coliCL membranes with cyt c_3, (*C*) coliPC/coliCL (4:1 w/w) membranes, and (*D*) coliPC/coliCL membranes with cyt c_3.

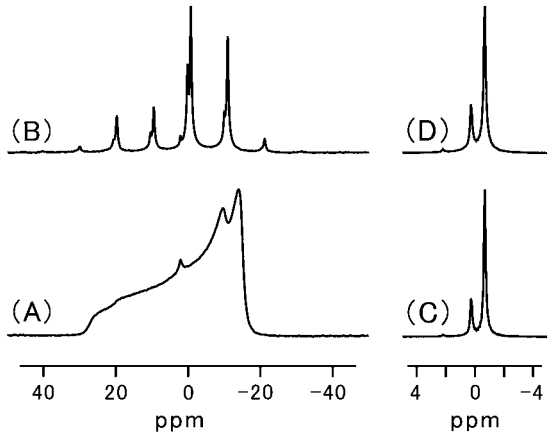

FIGURE 5 Proton decoupled ^{31}P-NMR spectra of doPC/beefCL (4:1 w/w) membranes with cyt c_3. (*A*) Powder pattern and (*B*) MAS spectrum (at 2 kHz spinning rate) and isotropic regions of the MAS spectra at spinning rate of 4 kHz (*C*) and 8 kHz (*D*). The signals at high, intermediate, and low fields are assigned to PC, CL, and the isotropic component, respectively, in *C* and *D*.

pattern appeared on binding of cyt c_3. This was remarkable in the case of PC/CL liposomes. Furthermore, the spectrum of PC/CL membranes clearly consists of two axially symmetric powder patterns with different chemical shift anisotropies (CSA $= |\sigma_{\perp} - \sigma_{//}|$), as can be seen in Fig. 4, *C* and *D*. CSA was determined by reading the chemical shifts at the half heights of the 90° and 0° discontinuities of the powder pattern. The powder patterns with large and small CSA can be ascribed to PC and CL, respectively, according to previous reports (14,23–26). Binding of cyt c_3 increased CSA of CL from 31 to 33 ppm for CL membranes and from 33 to 34 ppm for PC/CL membranes. In contrast, CSA of PC decreased from 49 to 47 ppm on binding of cyt c_3. Thus, both PC and CL are involved in the binding of cyt c_3 to PC/CL membranes. Since the changes in CSA on binding of cyt *c* to PC/CL membranes were subtle despite the similar protein/lipid ratios (14,23), the mode of interaction with the membranes containing CL differs for cyt c_3 and cyt *c*.

Binding of cyt c_3 induced a significant amount of an isotropic component. To clarify the role of this component, MAS ^{31}P NMR spectra were obtained for dioleoylphosphatidylcholine (doPC)/beefCL membranes. In contrast to the case mentioned above, only a small amount of the isotropic component was seen in the ^{31}P powder pattern spectrum (Fig. 5 *A*). Therefore, the isotropic component should not represent the essential structure induced by the binding of cyt c_3. MAS at a relatively low spinning rate (2 kHz) caused the axially symmetric powder pattern to collapse into a set of central isotropic signals and a series of rotational side bands (Fig. 5 *B*). MAS at higher spinning rates (4 and 8 kHz) gave rise to well-resolved isotropic signals of beefCL and doPC (Fig. 5, *C* and *D*). Assignment of the isotropic signals has already been reported (23). The intensities of these signals also closely reflected their chemical proportions, i.e., 4:1, in the lipid mixture, supporting the assignment. The isotropic signal in the powder pattern (Fig. 5 *A*) remained isolated downfield even in the MAS spectra. This suggests that the environment of the lipids contributing to the isotropic signal in the powder pattern is different from that in the major cyt c_3-bound liposomes. Anyhow, this fraction would not be important for electron transport, because the amount does not depend on that of cyt c_3.

Characterization of cyt c_3-membrane interactions by means of deuterium quadrupole splittings of the CL glycerol backbones

The interaction of cyt c_3 with deuterated cardiolipin (coliCL*) in membranes was examined by means of ^{2}H NMR. Fig. 6 presents solid-state ^{2}H NMR spectra of coliCL* and coliPC/coliCL* liposomes in the absence and presence of bound cyt c_3 at 35°C. The samples were the same as those used for ^{31}P NMR measurements. The assignments of the signals are given in Fig. 6 (19,27). In the spectra of CL* and PC/CL* liposomes without cyt c_3 (Fig. 6, *A* and *C*, respectively), the line width of the latter is broader than that of the former, suggesting that the environment of each CL molecule is more diverse in PC/CL* membranes than in CL* membranes on the timescale for the line shape. The ^{2}H NMR spectra of the CL* and PC/CL* membranes with bound cyt c_3 (Fig. 6, *B* and *D*, respectively) show that although the quadrupole splittings of the head glycerol deuterons of CL* hardly changed, those of the 3S and 2 &3R deuterons of the glycerol backbone became larger by ~1 and 0.5 kHz on binding of cyt c_3 to the membranes, respectively (3S, from 24.4 to 25.3 kHz for CL* and from 24.0 to 25.2 kHz for PC/CL*; and 2 and 3S, from 21.8 to 22.5 kHz for CL* and from 21.4 to 22.0 kHz for PC/CL*). The increases in the quadrupole splittings are in contrast to their decreases on

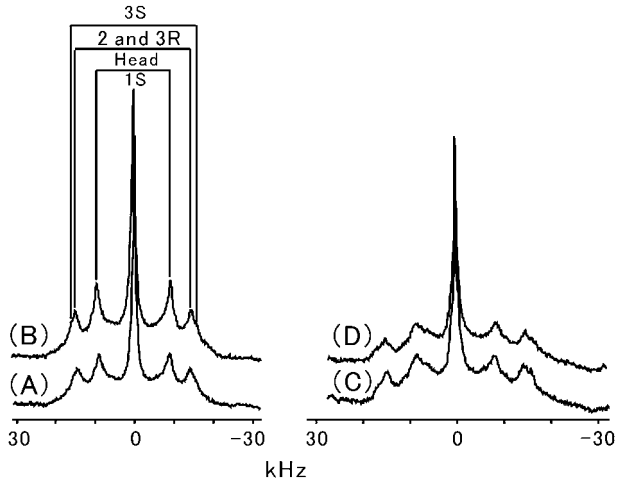

FIGURE 6 ^{2}H-NMR spectra of the deuterated CL glycerol backbone in coliCL* and coliPC/coliCL* membranes with and without cyt c_3 at 61.1 MHz and 35°C. (*A*) coliCL* membranes, (*B*) coliCL* membranes with cyt c_3, (*C*) coliPC/coliCL* (4:1 w/w) membranes, and (*D*) coliPC/coliCL* membranes with cyt c_3. Here, a lipid with asterisk denotes a deuterated one.

binding of cyt *c* to coliPC/coliCL membranes (14). The ^{2}H NMR spectra obtained at 30°C, 35°C, 40°C, and 45°C showed similar features (data not shown).

DISCUSSION

Nature of the electron transport mediated by cyt c_3

This work has confirmed cyt c_3-mediated electron transport across membranes. This can be ascribed to the high heme density of cyt c_3 and its stronger interaction with membranes. Furthermore, there are two reaction processes for cyt c_3-mediated electron transport, depending on the acidic phospholipid species and the membrane fluidity. Whereas a two-molecule process operates in PC/CL membranes in the liquid-crystalline state, a single-molecule process dominates in PC/CL membranes in the gel state and in PC/PG membranes in the liquid-crystalline and gel states. Since the electron transport rate constants for the three single-molecule processes are similar to each other, the rate-limiting step in the electron transport should be the same. It should comprise direct electron transfer from cyt c_3 to $Fe(CN)_6^{3-}$. The involvement of flip-flop of phospholipid molecules induced by cyt c_3 is unlikely for the single-molecule process because of the similar rate constants in the liquid-crystalline and gel states. On the other hand, the rate-limiting step in the alternative process is the lateral diffusion of cyt c_3. An encounter between two cyt c_3 molecules should induce electron transfer from cyt c_3 to $Fe(CN)_6^{3-}$. Tabushi and his colleagues proposed that pore formation by two cyt c_3 molecules mediates electron transport across PC/CL membranes in the liquid-crystalline state (7). However, this model is unlikely because even cyt c_3-bound PC/CL membranes showed the single-molecule electron transport process in the gel state. Furthermore, to make the Tabushi model possible, cyt c_3 has to be transported to inside of the membranes, crossing the hydrophobic area, which would be difficult in view of the hydrophilic nature of cyt c_3. The origin of the difference in the electron transport mechanism should be ascribed to the nature of the cyt c_3-membrane interaction.

Nature of the cyt c_3-membrane interaction

^{31}P NMR can provide information on the interaction between cyt c_3 and polar headgroups on the membrane surface. In general, residual CSA includes contributions from the molecular order and local conformation. Since the directions of the changes in ^{31}P CSA were opposite for CL and PC, it can be said that conformational changes in phosphate groups were induced on binding of cyt c_3. In the case of cyt *c* binding, the changes in ^{31}P CSA were subtle (14,23). Therefore, the modes of binding of cyt c_3 and cyt *c* should be significantly different, which is consistent with inability of cyt *c* to mediate electron transport across membranes. A large increase in ^{31}P CSA was observed for CL membranes on binding of cyt c_3. In contrast, the change in CSA of CL in PC/CL membranes was smaller. However, this does not mean that the effect of cyt c_3 binding is small in the latter. PC and CL form their own microdomains in PC/CL membranes, some CL molecules being incorporated into the PC microdomain (28). The interaction with PC induces an increase in CSA of CL, reflecting adaptation of CL to the conformation of PC, which gives a larger ^{31}P CSA. This would explain the smaller increase in CL CSA on binding of cyt c_3 to PC/CL membranes. In view of the involvement of PC in cyt c_3 binding, it affects a certain area around the binding site.

The deuterium quadrupole splittings of the CL glycerol backbone provide information on the interaction of cyt c_3 with the interface between the polar surface and hydrophobic core of the lipid membrane. The quadrupole splittings of the deuterated glycerol backbone of dmPC membranes were investigated comprehensively by Strenk et al. (27), who showed that the quadrupole splittings included contributions from the molecular order and the local conformation, and that the conformation of the glycerol backbone is relatively rigid. Since most quadrupole splittings increased on binding of cyt c_3, they should include an increase in the molecular order. This would be due to suppression of the mobility of the glycerol backbone induced by the presence of cyt c_3. This strongly suggests that cyt c_3 penetrates into a membrane deeper than the glycerol backbone, namely, into the hydrophobic region.

Proposed mechanisms for the cyt c_3-specific electron transport across membranes

Judging from our results, the following models explain the different electron transport mechanisms. When cyt c_3 binds

to the outside of a membrane, the bound cyt c_3 penetrates into the membrane a little deeper than the glycerol backbone in the outer leaflet but not to the inner leaflet in either PC/CL or PC/PG membranes. This penetration would perturb the structure of the inner leaflet of the bilayer. Namely, if the penetration is not deep enough to reach the inner leaflet, the structure of the inner leaflet should be distorted to compensate for the absence of lipids in the outer leaflet, as shown in Fig. 7. The hydrophobic properties of the exposed parts of the four hemes of cyt c_3 would make this possible. Actually, the exposure of every heme of cyt c_3 is much greater than that of cyt c (4). When the distortion of the inner layer is significant, $Fe(CN)_6^{3-}$ can penetrate into a membrane and gain access to the cyt c_3 surface in the membrane. This explains the single-molecule reaction process in the cyt c_3-bound PC/PG membrane system (Fig. 7 *A*). In the case of PC/CL membranes, however, the distortion of the inner bilayer structure is not enough for $Fe(CN)_6^{3-}$ to gain access to the cyt c_3 surface in a membrane. The stiffness of the CL molecule will help the inner layer maintain its integrity despite the perturbation induced by cyt c_3 binding (Fig. 7 *B*). It has been reported that PG membranes are flexible and easily form a highly curved surface (18). In contrast, CL membranes are stiff and PC ones show intermediate flexibility (18). An encounter between two cyt c_3 molecules in the outer leaflet will cause more distortion of the inner leaflet of membranes (Fig. 7 *C*). This allows $Fe(CN)_6^{3-}$ to penetrate into the inner leaflet and to gain access to cyt c_3 in the membrane. This explains the two-molecule reaction process observed for cyt c_3-bound PC/CL membranes in the liquid-crystalline state. In the gel state, however, the membranes are not flexible or fluid anymore. Thus, cyt c_3 will induce structural defects in the inner leaflet because of the rigid lipid structure, which enables $Fe(CN)_6^{3-}$ to gain access to cyt c_3 in the membrane. This may be why the three single-molecule processes showed similar second-order rate constants (Table 1). With the use of phospholipids deuterated at the hydrocarbon chain, ^{2}H-NMR would provide information on the distortion of the hydrocarbon chains. This remains for future investigation.

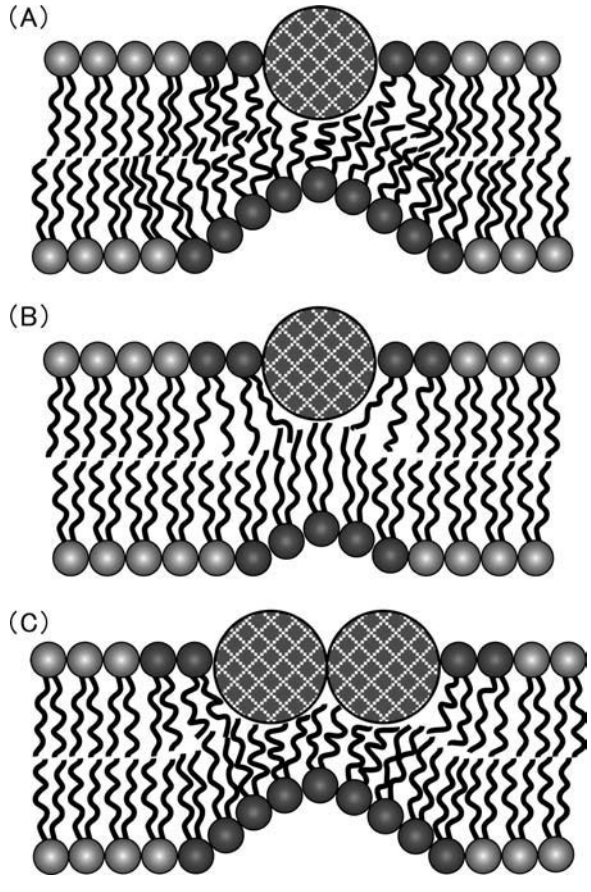

FIGURE 7 Schematic models of cyt c_3-bound membranes. (*A*) Cyt c_3-bound PC/PG membrane in the liquid-crystalline state, (*B*) cyt c_3-bound PC/CL membrane in the liquid-crystalline state, and (*C*) encounter between two cyt c_3 molecules in the PC/CL membrane in the liquid crystalline state. Dark spheres in lipid molecules indicate the polar groups of which the structures are perturbed on binding of cyt c_3.

This research was partly supported by a grant from the Ministry of Education, Science, Technology, Sport, and Culture of Japan (Grant-in-Aid for Scientific Research on Priority Areas and CREST) to H.A.

REFERENCES

1. Odom, J. M., and R. Singleton, editors. 1993. The Sulfate-Reducing Bacteria: Contemporary Perspectives. Springer-Verlag, New York.
2. Postgate, J. R. 1984. The Sulfate-Reducing Bacteria, 2nd ed. Cambridge University Press, Cambridge, UK.
3. Takayama, Y., E. Harada, R. Kobayashi, K. Ozawa, and H. Akutsu. 2004. Roles of non-coordinated aromatic residues in redox regulation of cytochrome c_3 from *Desulfovibrio vulgaris* Miyazaki F. *Biochemistry*. 43:10859–10866.
4. Ozawa, K., Y. Takayama, F. Yasukawa, T. Ohmura, M. A. Cusanovich, Y. Tomimoto, H. Ogata, Y. Higuchi, and H. Akutsu. 2003. Role of the aromatic ring of Tyr43 in tetraheme cytochrome c_3 from *D. vulgaris* Miyazaki F. *Biophys. J.* 85:3367–3374.
5. Fan, K., H. Akutsu, Y. Kyogoku, and K. Niki. 1990. Estimation of microscopic redox potential of a tetraheme protein, cytochrome c_3 of *D. vulgaris* Miyazaki F and partial assignments of heme groups. *Biochemistry*. 29:2257–2263.
6. Park, J.-S., T. Ohmura, T. Sagara, K. Niki, Y. Kyogoku, and H. Akutsu. 1996. Regulation of the redox order of four hemes by pH in cytochrome c_3 from *D. vulgaris* Miyazaki F. *Biochim. Biophys. Acta*. 1293:45–54.
7. Tabushi, I., T. Nishiya, T. Yagi, and H. Inokuchi. 1981. Efficient electron channel through self-aggregation of cytochrome c_3 on an artificial membrane. *J. Am. Chem. Soc.* 103:6963–6965.
8. Tabushi, I., T. Nishiya, T. Yagi, and H. Inokuchi. 1983. Kinetic study on the successive four-step reduction of cyt c_3. *J. Biochem. (Tokyo)*. 94:1357–1385.
9. Tabushi, I., T. Nishiya, M. Shimomura, T. Kunitake, H. Inokuchi, and T. Yagi. 1984. Cytochrome c_3 modified artificial liposome. Structure, electron transport, and pH gradient generation. *J. Am. Chem. Soc.* 106:219–226.
10. Tuominen, E. K. J., C. J. A. Wallace, and P. K. J. Kinnunen. 2002. Phospholipid-cytochrome *c* interaction. *J. Biol. Chem.* 277:8822–8826.
11. Zucchi, M. R., O. R. Nascimento, A. Faljoni-Alario, T. Prieto, and I. Nantes. 2003. Modulation of cytochrome *c* spin states by lipid acyl

chains: a continuous-wave electron paramagnetic resonance (CW-EPR) study of heme iron. *Biochem. J.* 370:671–678.

12. Oellerich, S., S. Lecomte, M. Paternostre, T. Heimburg, and P. Hildebrandt. 2004. Peripheral and integral binding to phospholipids vesicles. *J. Phys. Chem. B.* 108:3871–3878.
13. Florens, L., M. Ivanova, A. Dolla, M. Czjzek, R. Haser, R. Verger, and M. Bruschi. 1995. Interfacial properties of the polyheme cytochrome c_3 superfamily from *Desulfovibrio. Biochemistry.* 34:11327–11334.
14. Kim, S., K. Shin, T. Fujiwara, and H. Akutsu. 1998. The interaction of ferric and ferrous cytochrome c with cardiolipin in phospholipid membranes studied by solid-state ^{2}H and ^{31}P NMR. *J. Mol. Struct.* 441:183–188.
15. Park, J.-S., K. Kano, Y. Morimoto, Y. Higuchi, N. Yasuoka, M. Ogata, K. Niki, and H. Akutsu. 1991. ^{1}H NMR studies of ferricytochrome c_3 from *D. vulgaris* Miyazaki F and its interaction with ferredoxin I. *J. Biomol. NMR.* 1:271–282.
16. Ozawa, K., A. L. Tsapin, K. H. Nealson, M. A. Cusanovich, and H. Akutsu. 2000. Expression of a tetraheme, *D. vulgaris* Miyazaki F cytochrome c_3, in Shewanella oneidensis MR-1. *Appl. Environ. Microbiol.* 66:4168–4171.
17. Akutsu, H., Y. Suezaki, W. Yoshikawa, and Y. Kyogoku. 1986. Influence of metal ions and a local anesthetic on the conformation of the choline group of phosphatidylcholine bilayers studied by Raman spectroscopy. *Biochim. Biophys. Acta.* 854:213–218.
18. Yoshikawa, W., H. Akutsu, Y. Kyogoku, and Y. Akamatsu. 1985. An essential role of phosphatidylglycerol in the formation of osmotically stable liposomes of *Escherichia coli* phospholipids. *Biochim. Biophys. Acta.* 821:277–285.
19. Yoshikawa, W., H. Akutsu, Y. Kyogoku, and Y. Akamatsu. 1988. A ^{2}H-NMR study on the glycerol backbone of phospholipids extracted from *Escherichia coli* group under high osmotic pressure: evidence for multiconformations of phosphatidylethanolamine. *Biochim. Biophys. Acta.* 944:321–328.
20. Gerlach, E., and B. Deuticke. 1963. Eine einfache Methode zure Mikrobestimmung von Phosphat in der Papierchromatographie. *Biochem. Z.* 337:477–479.
21. Sagara, T., T. Koide, H. Saito, H. Akutsu, and K. Niki. 1992. Determination of the molar absorption coefficients of *c*-type cytochromes using optically transparent thin-layer electrodes. *Bull. Chem. Soc. Jpn.* 65:424–429.
22. Akutsu, H., J. H. Hazzard, R. G. Bartsch, and M. A. Cusanovich. 1992. Reduction kinetics of the four hemes of cytochrome c_3 from *Desulfovibrio vulgaris* by flash photolysis. *Biochim. Biophys. Acta.* 1140:144–156.
23. Spooner, P. J. R., and A. Watts. 1992. Cytochrome c interaction with cardiolipin in bilayers: a multinuclear magic-angle spinning NMR study. *Biochemistry.* 31:10129–10138.
24. Ghosh, R. 1988. ^{31}P and ^{2}H NMR studies of structure and motion in bilayers of phosphatidylcholine and phosphatidylethanolamine. *Biochemistry.* 27:7750–7758.
25. Marassi, F. M., and P. M. Macdonald. 1991. Response of the headgroup of phosphatidylglycerol to membrane surface charge as studied by deuterium and phosphorus-31 nuclear magnetic resonance. *Biochemistry.* 30:10558–10566.
26. Shin, K., T. Fujiwara, and H. Akutsu. 1995. Modulation of the specific interaction of cardiolipin with cytochrome c by zwitterionic phospholipids in binary mixed bilayers; a ^{2}H and ^{31}P NMR study. *J. Mol. Struct.* 55:47–53.
27. Strenk, L. M., P. W. Westerman, and J. W. Doane. 1985. A model of orientational ordering in phosphatidylcholine bilayers based on conformational analysis of the glycerol backbone region. *Biophys. J.* 48:765–773.
28. Shin, K., H. Maeda, T. Fujiwara, and H. Akutsu. 1995. Molecular miscibility of phosphatidylcholine and phosphatidylethanolamine in binary mixed bilayers with acidic phospholipids studied by ^{2}H and ^{31}P NMR. *Biochim. Biophys. Acta.* 1238:42–48.